The electronic structure of UCoGe by *ab initio* calculations and XPS experiment

2010 J. Phys.: Condens. Matter 22 015503

(http://iopscience.iop.org/0953-8984/22/1/015503)

J. Phys.: Condens. Matter **22** (2010) 015503 (11pp) doi:10.1088/0953-8984/22/1/015503

The electronic structure of UCoGe by *ab initio* calculations and XPS experiment

M Samsel-Czekała[1,2], S Elgazzar[3,4], P M Oppeneer[4], E Talik[5], W Walerczyk[2] and R Troć[2]

[1] Leibniz-Institut für Festkörper- und Werkstoffforschung, IFW Dresden, PF 270116, D-01171 Dresden, Germany
[2] Institute of Low Temperature and Structure Research, Polish Academy of Sciences, PO Box 1410, 50-950 Wrocław 2, Poland
[3] Department of Physics, Faculty of Science, Menoufia University, Shebin El-kom, Egypt
[4] Department of Physics and Materials Science, Uppsala University, Box 530, S-751 21 Uppsala, Sweden
[5] Institute of Physics, University of Silesia, Uniwersytecka 4,40-007 Katowice, Poland

E-mail: m.samsel@int.pan.wroc.pl

Received 8 September 2009, in final form 12 November 2009
Published 8 December 2009
Online at stacks.iop.org/JPhysCM/22/015503

Abstract
The crystal and electronic structures of the orthorhombic compound UCoGe are presented and discussed. It has been either refined by the x-ray diffraction on a single crystal or computed within the local spin density functional theory, employing the fully relativistic version of the full-potential local-orbital band structure code, respectively. We particularly give our attention to investigating the Fermi surface and de Haas–van Alphen quantities of UCoGe. The calculated electronic density is then examined by x-ray photoelectron spectroscopy (XPS). Fairly good agreement is achieved between theoretical and experimental XPS results in the paramagnetic state. A small difference in the position (in energy scale) of the U 5f bands is caused by the electron localization effect observed in the experimental XPS. There is also some discrepancy for the Co 3d electron contributions below E_F. The Fermi surface in the non-magnetic state is of a semimetallic type while that in the ferromagnetic state, with the ordered moment of $-0.47\ \mu_B$/f.u. along the c axis, is more metallic, with nesting properties that may favour superconductivity.

(Some figures in this article are in colour only in the electronic version)

1. Introduction

In recent years UCoGe has attracted much attention, as it was reported to become superconducting in a weakly ferromagnetic state [1–3]. It crystallizes in a very common crystal structure of the orthorhombic TiNiSi type (space group: *Pnma*) as do also many other uranium germanides of the composition UTGe (where T is a transition metal). They exhibit a variety of magnetic properties such as paramagnetism down to the lowest temperatures, and an antiferro- or ferromagnetic order [4]. In this type of structure the U atoms are arranged in characteristic zigzag chains along the a axis. This complicates the formation of magnetic ordering in the TiNiSi-type lattice due to the effect of the pseudo-one-dimensional structure. Previously, several measurements of the lattice parameters of UCoGe have been made on polycrystalline [1, 2, 4] and on single-crystalline [5] samples; the results are quite similar to one another. Up to now, the x-ray refinement of atomic positions has been given only in [5]. With the purpose of assessing the quality of our single crystal separated from the bulk sample of UCoGe we present here the results of our x-ray refinement, as well.

In the past, measurements of the susceptibility and electrical resistivity of polycrystalline UCoGe were performed down to 4.2 K [4, 6] as well as specific heat measurements down to 1.2 K [7]. On the basis of these measurements, this compound was considered to be a paramagnetic system down to 4.2 K. However, after the discovery by Huy *et al* [1] of superconductivity coexisting with some weak ferromagnetism below 0.8 K at ambient pressure, several intensive studies have been performed recently. Low

temperature magnetic and transport experiments were carried out on both polycrystalline [2, 8, 9] and single-crystalline [3] samples. So far, there have been no reports on XPS measurements.

To the best of our knowledge, only two rather brief reports were recently published for UCoGe, containing limited band structure calculation results based on the full relativistic full-potential local-orbital (FPLO) minimum basis code and the WIEN2k package within the local (spin-) density approximation (L(S)DA) [10] as well as the WIEN2k within LSDA $+U$ [11] methods. Our band structure results for UCoGe are obtained employing two different versions of the FPLO code, namely FPLO5 [12] and RFPLO [13] within L(S)DA and with and without orbital polarization correction (OPC). The calculations are based on lattice parameters and atomic positions reported in this work that are refined on a single-crystalline sample. In addition, we present not only densities of states (DOSs) but also Fermi surfaces (FSs) and de Haas–van Alphen (dHvA) quantities, band energies, $E_n(\mathbf{k})$, and band weights, occupation numbers, and values of ordered magnetic moments in the ferromagnetic state determined along three main crystallographic orientations. We also compare our computed results with experimental x-ray photoelectron spectroscopy (XPS) data, which we obtained on an (as grown) single crystal of UCoGe. Differences between our and the previously published band structure results [10, 11] are carefully discussed.

Table 1. Crystallographic data and structure refinement parameters obtained for UCoGe.

Structure parameters	Room-temperature data
Empirical formula	Co Ge U
Formula weight	369.55
Temperature	293(2) K
Wavelength	0.071 073 nm
Crystal system, space group	Orthorhombic, *Pnma*
Unit cell dimensions	$a = 0.684\,72(14)$ nm, $\alpha = 90°$ $b = 0.421\,09(8)$ nm, $\beta = 90°$ $c = 0.722\,96(14)$ nm, $\gamma = 90°$
c/a	1.05585
b/a	0.61498
Volume	$0.208\,45(7)$ nm^3
Z, calculated density	4, 11.776 mg m^{-3}
Absorption coefficient	99.189 mm^{-1}
F (000)	604
Reflections collected/unique	3776/598 [R(int) = 0.0755]
θ range for data collection	4.10°–37.77°
Limiting indices	$-10 \leqslant h \leqslant 11$, $-5 \leqslant k \leqslant 7$, $-12 \leqslant l \leqslant 8$
Completeness to $\theta = 37.77$	96.6%
Refinement method	Full-matrix least-squares on F^2
Data/restraints/parameters	598/0/20
Goodness of fit on F^2	1.110
Final R indices ($I > 2\sigma(I)$)	$R_1 = 0.0447$, $wR_2 = 0.1192$
R indices (all data)	$R_1 = 0.0607$, $wR_2 = 0.1260$
Extinction coefficient	0.0108(14)
Largest diff. peak and hole	10 242 and -7675 e nm^{-3}

2. Experiment

A polycrystalline sample in a form of a button was prepared by arc melting the high purity constituents under argon atmosphere. A single-crystalline rod of UCoGe was pulled out from the melt of the button using a radio frequency furnace in the Czochralski technique. The starting elements (with purity in weight per cent) were U (99.98), Co (99.99), and Ge (99.999). No further heat treatment of the sample was performed.

A single-crystal x-ray refinement was performed at room temperature on an Xcalibur 2 four-circle diffractometer equipped with a CCD camera using graphite-monochromatized Mo Kα radiation. The intensities of reflections were corrected for Lorentz and polarization effects. The crystal data were refined by the full least-squares method using the SHELX-97 program [14].

For XPS measurements a cylindrical sample of typical dimension $\phi = 1.0$ mm and $l = 5.0$ mm was used. The XPS spectrum was recorded at room temperature in a Physical Electronics PHI 5700/660 photoelectron spectrometer using a monochromatized Al Kα x-ray source ($h\nu = 1486.6$ eV) [15]. The angle between the x-ray beam and the sample surface was 45°. All measurements were performed under ultra-high vacuum (UHV) conditions (in the range 10^{-10} Torr), immediately after the surface of the UCoGe sample had been obtained by cleaving the (100) planes *in situ*. The energy spectra of the electrons were analysed by a hemispherical mirror analyser with an energy resolution of 0.3 eV. The Fermi level (E_F) was referenced to the binding energy of the 4f states of gold at 84 eV. The single-crystalline sample of UCoGe, after breaking in UHV conditions, produced an overall spectrum with only negligible oxygen and carbon contaminations. In the whole region of the measured spectrum (−1400–1 eV) there are only small traces of O (KLL) and C (1s) at −975 and −290 eV, respectively. The distinct O (2s) peak near −6 eV is also lacking. The probed single crystal turned out to be quite stoichiometric (1:1:1) and did not show signs of surface degradation during the XPS experiment.

3. Theory

The band structure of UCoGe has been computed using the fully relativistic versions of the FPLO method FPLO5 [12] and RFPLO [13]. In this method the four-component Kohn–Sham–Dirac equation, containing implicitly spin–orbit coupling up to all orders, is solved self-consistently. The Perdew–Wang parametrization [16] of the exchange–correlation potential in the L(S)DA with and without OPC [17] approach was utilized. For the calculations our experimental values at room temperature of lattice parameters and atomic positions in the unit cell (u.c.) were used from tables 1 and 2. The adopted valence basis sets were as follows: the U 5d5f;6s6p6d;7s7p, Co 3s3p3d;4s4p, and Ge 3s3p3d;4s4p states. The higher-lying 5d6s6p semicore uranium states that have a possibility of hybridizing with the 6d and 5f valence states were also included in the basis. The maximum size of the **k**-point mesh in the Brillouin zone was $20 \times 20 \times 20$, though the $12 \times 12 \times 12$ mesh turned out to be sufficient.

Table 2. Atomic coordinates, anisotropic and equivalent isotropic displacement parameters ($nm^2 \times 10$) for UCoGe.

Atom	Site	X	Y	Z	U_{11}	U_{22}	U_{33}	U_{13}	$U^a_{(eq)}$
U	4c	0.0098(6)	1/4	0.7075(5)	3(1)	3(1)	9(1)	0(1)	5(1)
Co	4c	0.2891(4)	1/4	0.4181(4)	16(1)	4(1)	9(1)	1(1)	10(1)
Ge	4c	0.1964(3)	1/4	0.0871(3)	6(1)	3(1)	9(1)	0(1)	6(1)

[a] $U_{(eq)}$ is defined as one-third of the trace of the orthogonalized U_{ij} tensor. The anisotropic displacement factor exponent takes the form $-2\pi^2[h^2a^{*2}U_{11} + \cdots + 2hka^*b^*U_{12}]$ and $U_{23} = U_{13} = 0$.

For both the non-magnetic and ferromagnetic states, the total energy values, band energies, $E_n(\mathbf{k})$, and chosen band weights and occupation numbers for different states, Fermi surfaces and dHvA quantities, as well as total and partial DOSs per formula unit (f.u.), have been calculated within the LDA and LSDA. Furthermore, spin and orbital polarized LSDA and LSDA + OPC calculations were performed for a ferromagnetic arrangement of magnetic moments along the a, b and c axes to evaluate possible values of ordered magnetic moments. The DOSs were computed for each atomic site in the u.c. (containing 4 f.u.) and for all atomic states considered separately. Based on the above partial DOSs in the non-magnetic (LDA) state, the theoretical valence band XPS spectrum was calculated by the following standard procedure. The partial DOSs (for each kind of state in the constituent atoms) were multiplied by the respective weight factors proportional to atomic subshell photoionization cross-sections [18] and the outputs were summed up and convoluted with a Gaussian of full width at half maximum 0.3, 0.4 and 0.6 eV to simulate the instrumental energy resolution of the experimental analyser. Usually, this value should be taken to be equal roughly to 0.3 eV. Finally, thus-calculated spectra were compared with the experimental spectrum measured at room temperature, i.e. in the paramagnetic state of UCoGe. The dHvA cyclotron frequencies F, which are proportional to the Fermi surface cross-sections, have been calculated numerically by discretizing the Fermi velocities on **k** points along the orbit and by a subsequent Romberg integration [19].

4. Results

4.1. Structure refinement

A full single-crystal x-ray refinement has been performed for UCoGe on data collected at room temperature. The results are given in tables 1–3. The crystal structure of UCoGe was refined with anisotropic displacement parameters (ADPs) for all atoms. It turns out that thus obtained atomic positions, next used in our calculations, are very similar to those given in [5], also found in a single-crystal refinement. Note that we, additionally, provide the ADPs (table 2), which are also visualized in figure 1, and the interatomic distances (table 3). The unit cell of UCoGe in the TiNiSi-type structure is displayed in figure 1, where the ADPs are presented in terms of ellipsoids together with the coordination of nearest neighbouring atoms around the centred uranium atom.

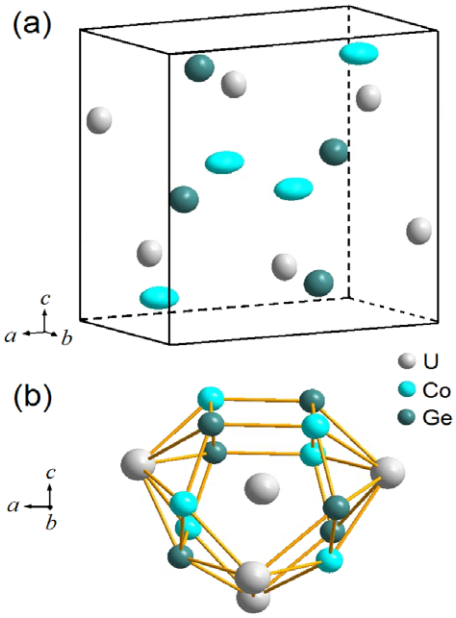

Figure 1. (a) The crystal unit cell of UCoGe of the TiNiSi-type (*Pnma*) structure with possible ADPs represented by ellipsoids; (b) coordination of nearest neighbouring atoms around a central uranium atom in UCoGe.

Table 3. Selected interatomic distances (nm) for UCoGe.

U–U	2× 3.4794(3)	U–Ge	1× 3.0258(4)
	2× 3.6703(1)		1× 3.0284(1)
			2× 3.0931(1)
			2× 3.9385(5)
U–Co	1× 2.8355(4)	Co-Ge	2× 2.4363(2)
	2× 2.9408(1)		1× 2.4772(3)
	2× 3.0749(3)		1× 2.7908(2)
	1× 3.1007(1)		

As seen from tables 2 and 3, the U, Co, and Ge atoms are located in position (4c) with the coordination number CN = 16 (4U + 6Co + 6Ge).

The interatomic distances, collected in table 3, indicate that the nearest U–U distance $d_{U-U} = 0.348$ nm is around the Hill limit of 0.35 nm. This fact puts this compound almost on the border between the localized ($d_{U-U} > 0.35$ nm) and itinerant ($d_{U-U} < 0.35$ nm) character of the 5f electrons, where one could expect a strong 5f–ligand hybridization due to the large coordination number of the uranium central atom, visualized in figure 1(b). As discussed in detail previously in [4], the extent of 5f–ligand hybridization in this compound is rather weak despite the small d_{U-U} distances (see table 1), due to the possibility to fill up almost completely the Co 3d shell by a transfer of electrons from the uranium atoms. Thus, this may yield a significantly localized behaviour of U 5f electrons in UCoGe, at least at higher temperatures. On the other hand, at low temperatures an expected shrinking of the crystal lattice may favour some extension of the 5f electron delocalization. The nearest U–Co and U–Ge distances are comparable to each other, amounting to about 0.294 nm.

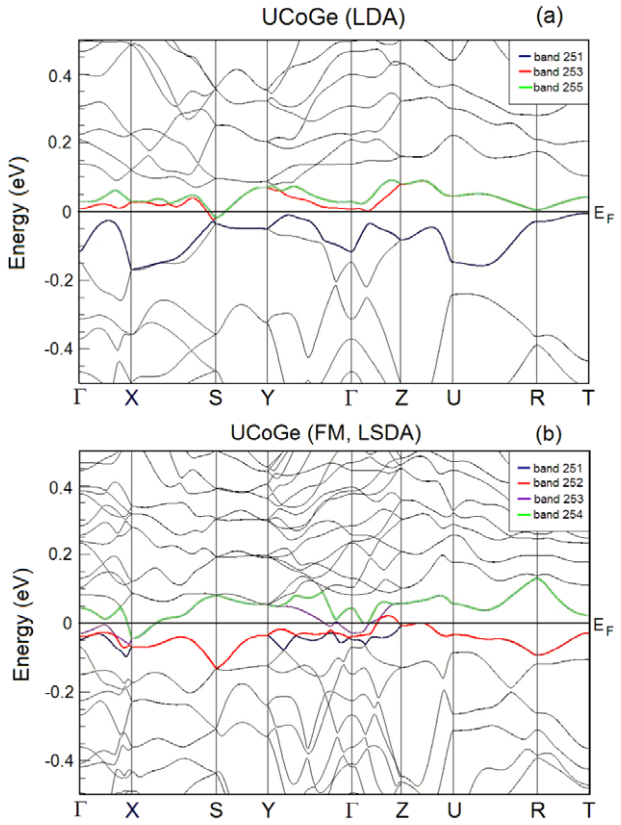

Figure 2. Relativistic energy bands $E_n(\mathbf{k})$ for UCoGe in the vicinity of E_F, for (a) non-magnetic and (b) ferromagnetic (FM) states, the latter case with magnetic moments arranged along the c axis.

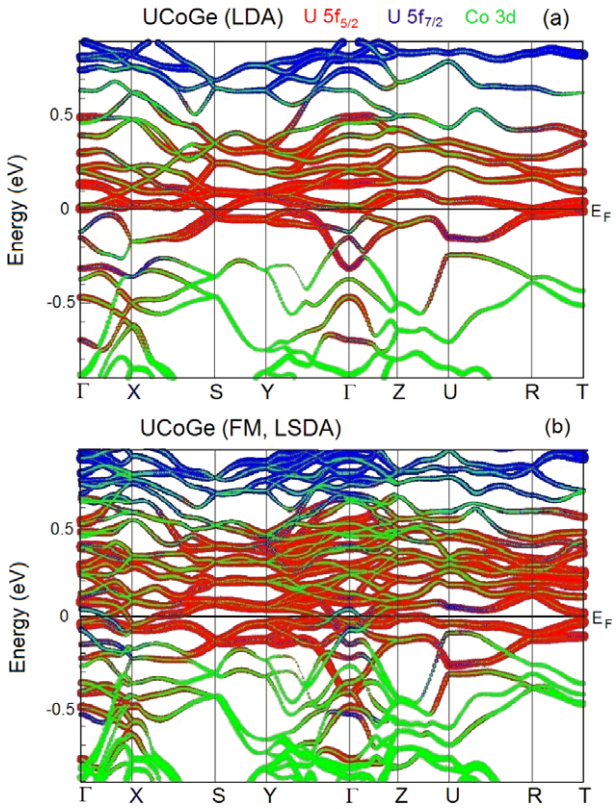

Figure 3. The character of the energy bands, in the vicinity of E_F, for UCoGe in (a) non-magnetic and (b) ferromagnetic states, the latter with moment along the c axis. The amounts of the U $5f_{5/2}$, U $5f_{7/2}$ and Co 3d state characters are marked by the different colours and thickness of the bands.

4.2. Electronic structure calculations and x-ray photoelectron spectroscopy

The theoretical band energies for both the non-magnetic and ferromagnetic states (the latter with magnetic moments along the c axis) of UCoGe (LDA and LSDA, respectively) are presented in figure 2. The corresponding selected band weights, namely weighted contributions of the U $5f_{5/2}$, U $5f_{7/2}$ and Co 3d states to the energy bands, are displayed in figure 3. It is seen from these figures that in the non-magnetic case there are three bands crossing the Fermi level (251, 253, 255). Each band is twofold Kramers degenerated, i.e. bands 251 and 252 are identical (the same for 253 and 254 or 255 and 256). In turn, in the ferromagnetic case four non-degenerated (251–254) bands cut E_F.

As seen from figure 2(a), the non-magnetic (LDA) bands exhibit typically semimetallic behaviour with a narrow band gap of 0.2 eV visible along several main symmetry directions, while the bands in the ferromagnetic state exhibit more metallic behaviour and then the gap either disappears or is reduced. The bands crossing E_F are dominated by the U $5f_{5/2}$ states (see figure 3), being partly hybridized with the Co 3d states, and these together create a metallic bond. The Co 3d states are clearly present in the whole range of valence band energies with some tail at E_F. However, the analysis of total and partial DOSs computed with FPLO, which are displayed in figures 4–6 for both non-magnetic and ferromagnetic UCoGe, shows that all three kinds of atom are also connected to one another by covalent bonds, especially due to their electrons in hybridized bands in the range of 8–10 eV below E_F. Moreover, some U 6d and Ge 4p band tails occur at E_F as well, also contributing to a metallic bond. In both the non-magnetic and ferromagnetic cases, the U 5f states have (relative to other uranium compounds) broad contributions in the energy scale, ranging from about 5.5 eV below E_F up to 5.0 eV above E_F. Additionally, a small trace of these states occurs in the range of 8–10 eV below E_F. Typically for other UTM compounds, the spin–orbit coupling leads to two main U 5f peaks, split into the $5f_{5/2}$ and $5f_{7/2}$ states (in energy range between -0.2 and 2.0 eV), shifted from each other by about 1 eV. The U $5f_{5/2}$ states cut the Fermi level at a minimum of their peak, which yields not so high DOS at E_F. The calculated value of the electronic specific heat coefficient is only about $\gamma_b = 8.9$ and 8.1 mJ K^{-2} mol^{-1} for the non-magnetic and ferromagnetic cases, respectively. The contribution of the Co 3d states is present in the same energy range as that of the U 5f states, but it dominates in the range of -4 to -1 eV. There is also a wide (flat) contribution from the U 6d and Ge 4p states in the same energy range as that of the U 5f states, hybridizing with the latter. In the non-magnetic state there is a pronounced hybridization pseudogap at -0.2 eV, which is remarkably reduced in the ferromagnetic state. The DOS in the latter state of the spin-up channel is several times higher than the DOS of the spin-down channel, having a pseudogap at E_F, and thus

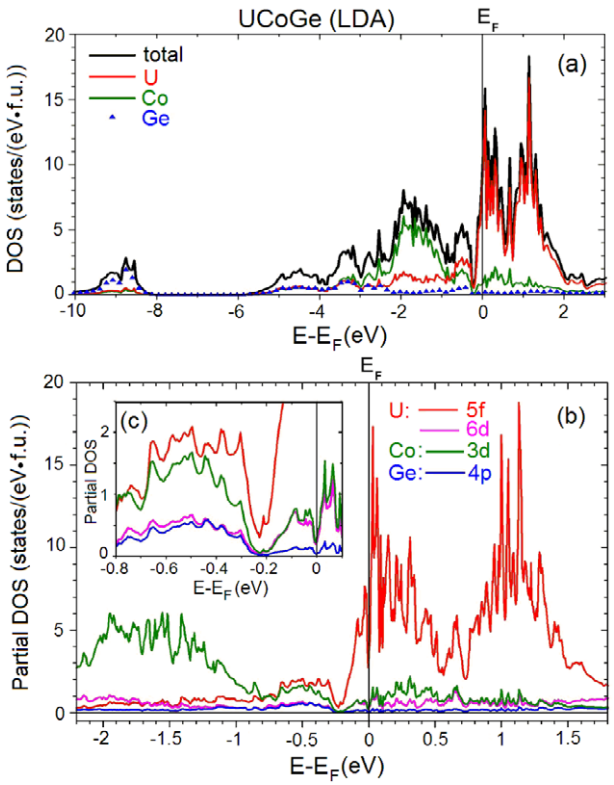

Figure 4. Calculated DOSs for UCoGe in the non-magnetic state: total and partial ones (on atomic sites) (a) as well as for different orbital states (b). The inset (c) shows the region around E_F on an expanded scale.

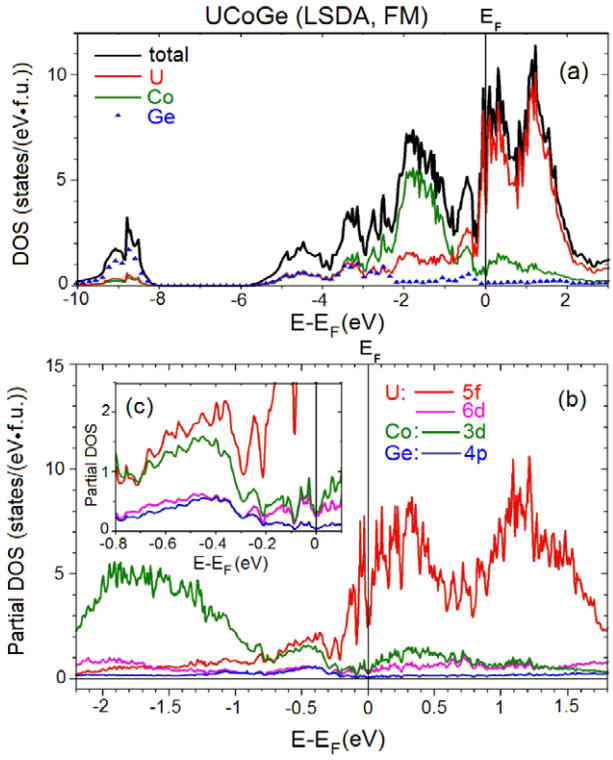

Figure 5. Calculated DOSs for UCoGe in the ferromagnetic (FM) state (along the c axis) with summed spin-up and spin-down channels: total and partial (on atomic sites) (a) as well as for different orbital states (b). The inset (c) shows the energy region around E_F on an expanded scale.

this compound can be regarded as being close to possessing the half-metallic feature. Interestingly, there are two small peaks of the U 5f spin-up states located just below E_F (the closest one to E_F occurs at -0.025 eV) that may cause some magnetic instabilities and lead to magnetic fluctuations as in RCo_2 compounds [20].

The electron population analysis of the non-magnetic UCoGe results gives the following occupation numbers (N). This number for the U 5f states is—in comparison to those of a free U atom—reduced from 3 to 2.84, for the U 6d states it is strongly enhanced from 1 to 2.38 electrons per atom, while for the U 7s states it is diminished from 2 to 0.5 electrons. Simultaneously, the U 7p states occur with non-negligible $N = 0.22$ electrons compared with $N = 0$ for the free atom occupation. In turn, the higher Co 4p states occur with high $N = 0.74$ at the cost of a remarkable reduction of N for the Co 4s states from 2 to 0.63. It is worthwhile underlining here that N for the Co 3d electrons is also strongly enhanced from 7 to 8 electrons. In the case of Ge, N of the 4s states is reduced from 2 to 1.45 and for 4p states it is increased from 2 to 2.19, while for the 3d states $N = 10$, remaining thus unchanged compared with that for a free atom. As a result, there is a large charge transfer of 0.68 valence electrons from U atoms to both Co (0.56) and Ge (0.13) atoms/f.u. The calculations for the ferromagnetic state yield charge transfers that are very similar to the above ones (the maximum difference is only equal to 0.02).

The Fermi surface of UCoGe calculated for both the non-magnetic (LDA) and ferromagnetic (LSDA) states (with moments along the c axis) is presented in figure 7.

The FS sheets of non-magnetic and ferromagnetic UCoGe (left- and right-hand panels, respectively) exist in three twofold Kramers degenerated (251, 253, 255) and four non-degenerated (251–254) bands, respectively. The non-magnetic FS sheets are strongly reduced—typically of a semimetal. The FS sheet in the first conduction band consists of four small hole shells with a shape typical of nesting (also called webbing) [21] along the c axis that may intermediate magnetic exchange interactions or superconductivity. The nesting vector $\mathbf{q}_1$ is marked in figure 7. The FS sheets in the two next conduction bands contain only small electron pieces: four long cigars in the corners of the Brillouin zone along the c axis accompanied by four small pockets in the middle of the Brillouin zone (about the Γ point) in the second band, as well as only extremely reduced cigars in the third one. These FS sheets located close to the high symmetry points Γ, R, and S are especially sensitive to a change of the Fermi level (see also figure 2(a)). Furthermore, the ferromagnetic FS sheets consist of four very small hole pockets in the first conduction band and two large longitudinal orthorhombic hole pieces with nesting properties along all three axes in the second band, marked by nesting vectors $\mathbf{q}_2$–$\mathbf{q}_4$. Moreover, there is an open electron cylindrical sheet along the a axis with nesting vector along the a axis, $\mathbf{q}_5$, in the third band, and there exist two plane electron discs

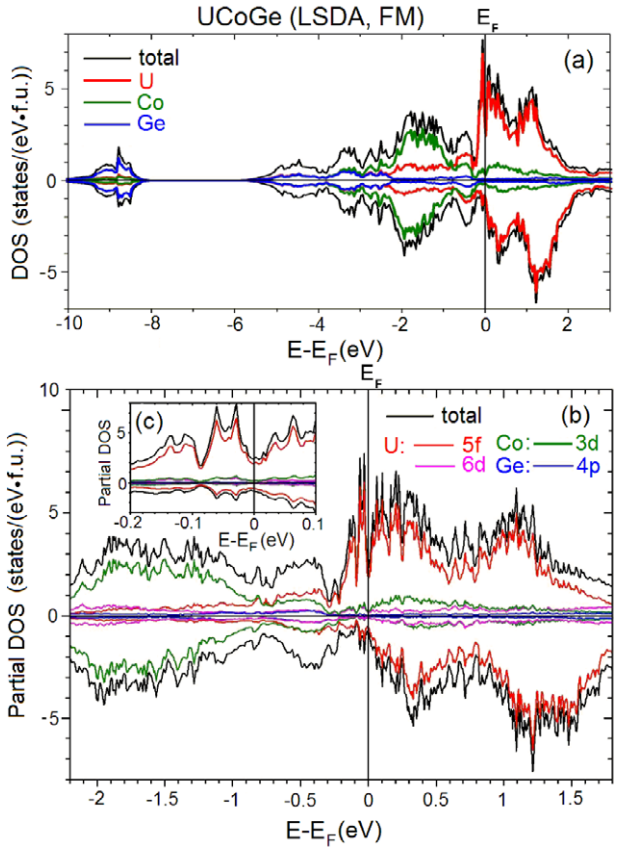

Figure 6. The same as in figure 5 but spin-up and spin-down channels are shown separately.

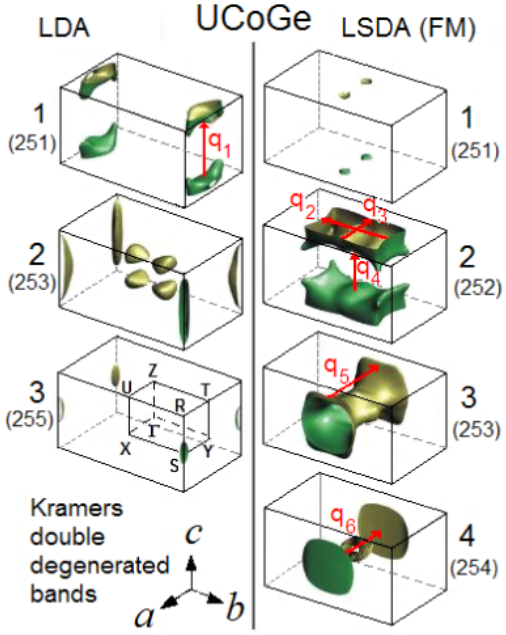

Figure 7. Calculated FS sheets of UCoGe in the non-magnetic (left-hand panel) and ferromagnetic (along the c axis) (right-hand panel) states, drawn separately for each band in the orthorhombic Brillouin zone with marked high symmetry points and possible nesting vectors $\mathbf{q}_1, \ldots, \mathbf{q}_6$ with respective lengths: 0.41 $(2\pi/c)$, 0.73 $(2\pi/b)$, 0.48 $(2\pi/a)$, 0.53 $(2\pi/c)$, 0.90 $(2\pi/a)$, 0.85 $(2\pi/a)$.

with the nesting vector $\mathbf{q}_6$ along the a axis and, finally, a small electron element in the middle of the Brillouin zone in the fourth band. The discs are unstable with even slight changes of lattice parameters (they are shifted from the third band). In a similar way, the electrons in the middle of the fourth Brillouin zone are also unstable. It is worth underlining that the ferromagnetic FS is typically metallic, with nesting properties along all axes that may favour both magnetism and/or superconductivity.

A detailed insight into the electronic structure can be gained from, e.g., dHvA measurements. Unfortunately, we are not aware of any dHvA experiments not only for UCoGe but also for the whole family of 1:1:1 uranium ternaries UT(Si, Ge). In an attempt to initiate possible experiments, we provide here dHvA frequencies and their angular dependences in both the non-magnetic and ferromagnetic states of UCoGe as a representative of the UT(Si, Ge) family. The extremal orbits have been calculated using the numerical scheme presented in [19], which outlined in detail an earlier work on this subject [22]. In tables 4 and 5 we gather calculated values of the dHvA frequencies F for the non-magnetic and ferromagnetic states of UCoGe, respectively. The extremal orbits for a magnetic field **H** orientation along the [001], [100] and [010] directions are displayed in figure 8 and labelled with Greek letters and corresponding band numbers.

The FS in the non-magnetic state (see figure 7) consists of four sheets and thus there are four extremal orbits for

Table 4. Calculated dHvA frequencies F (in kT) with $\mathbf{H} \parallel c$ for UCoGe in the non-magnetic state.

H	Orbits	Band no	Central point	Area (kT)
001	α	251	$\mathrm{T}'_{k\_b=0.70}$	0.747
	β	253	S	1.113
	γ	253	$\Gamma_{k\_c=0.15}$	0.362
	δ	255	S	0.213

Table 5. Calculated dHvA frequencies F (in kT) with $\mathbf{H} \parallel a$, $\mathbf{H} \parallel c$, and $\mathbf{H} \parallel b$ for UCoGe in the ferromagnetic state.

H	Orbits	Band no	Central point	Area (kT)
100	ρ	253	Γ	1.237
	ϕ	253	$X'_{k\_a=0.20}$	0.852
	μ	253	$X''_{k\_a=0.45}$	2.250
	λ	253	X	1.325
	ξ	254	X	1.295
001	χ	252	Z	0.270
	ω	252	Z	3.726
010	τ	252	Z	1.748
	η	252	$\mathrm{Z}'_{k\_a=0.16}$	1.442

a magnetic field along the c-axis direction. In table 4 the extremal orbits denoted as β and δ are connected with those FS sheets centred at the S point, while α and γ orbits correspond to those located close to the T and Γ points centred at **k** points (0.0, 0.70, 0.47) and (0.00 0.30 0.15), respectively. We expect that α and γ orbits are very sensitive to both the alignment of the magnetic field and purity of the crystal due to their shapes and locations. It is quite clear (see figure 7) that there are

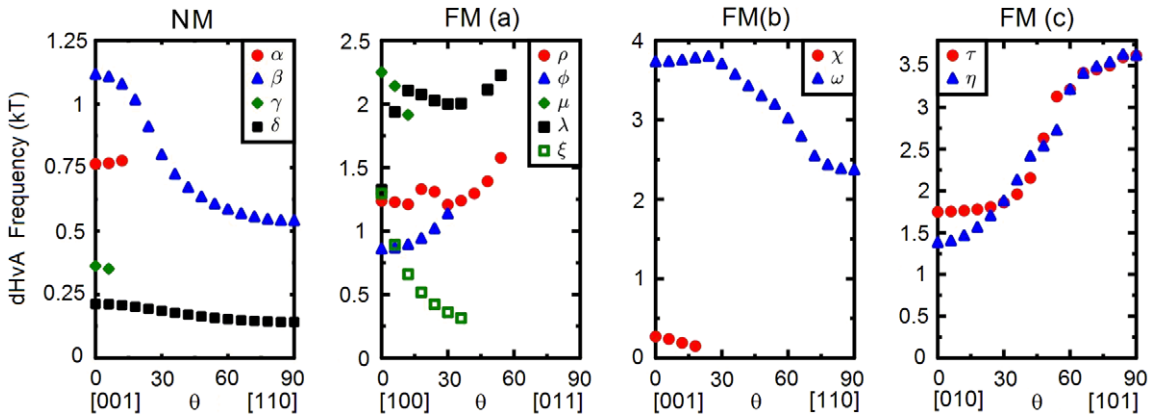

Figure 8. Calculated angular dependences of the dHvA frequencies of UCoGe in the non-magnetic (NM) for **H** ∥ [001] and ferromagnetic (FM) states, the latter case for different directions of the magnetic field: (a) **H** ∥ [100], (b) **H** ∥ [001] and (c) **H** ∥ [010].

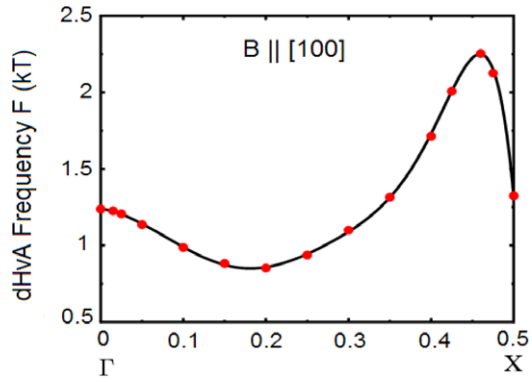

Figure 9. Calculated dHvA frequencies F with **H** ∥ a scanned along the ΓX line, where four extremal orbits occur in the ferromagnetic state.

considerable differences between FSs in the non-magnetic and ferromagnetic states. In the latter state we have four bands crossing the Fermi level, which are drawn in four separate Brillouin zone boundaries. For magnetic field orientations along the c and b axes we have four extremal orbits originating from the 252 band (see table 5). Three of them, centred close to the Z point, are denoted as χ, ω, and τ, while the fourth one, η, is centred at the Z′ with $\mathbf{k} = (0.00, 0.16, 0.47)$. The ω orbit has the largest frequency value among all dHvA orbits for both non-magnetic and ferromagnetic phases. Most of the dHvA frequencies arise from the 253 band when the field is directed along the a axis. As many as four extremal orbits are found in the case of scanning along the ΓX high symmetry line as shown in figure 9. Finally, the ξ orbit centred at the X point occurs in the 254 band. All corresponding values of frequencies are given in table 5.

Spin and orbital polarized self-consistent calculations, within both the LSDA and LSDA + OPC approximations, yielded very similar values of the ordered magnetic moments along the a, b and c axes. It was found that the arrangement of the moments along the c axis is slightly more favourable, having lower total energy (by about 0.6 and 1.2 mhartree) than that along the b and a axis alignment. Thus, the magnetocrystalline anisotropy is moderately small between all these axes. The difference in the values of total ordered magnetic moments between the results of LSDA and LSDA + OPC approximations, however, is as large as $\Delta\mu_{\mathrm{tot}} \approx 1.5\ \mu_{\mathrm{B}}$, also being comparable for all axes considered here. The total moments and their components for all three axes are given in table 6.

It is clear from table 6 that, in the case of LSDA calculations, the values of antiparallel spin and orbital moments on a uranium atom almost compensate each other. The spin and orbital moments on the Co atom are rather small, but parallel, and thus enhance each other, yielding about two to three times (depending on the given axis of magnetic alignment) larger total magnetic moment on the Co atom than on the U atom. Hence, the total moment per U atom aligned along the c, b, and a axes is as small as -0.14, -0.09, and $0.09\ \mu_{\mathrm{B}}$, respectively (note that only for the a axis is this value positive). At the same time, the Ge atom delivers a negligibly negative total magnetic moment. Finally, UCoGe has μ_{tot} (per f.u.) equal to about -0.47, -0.42, and $-0.24\ \mu_{\mathrm{B}}$, for alignments along the above three axes, respectively. The situation is completely changed when OPC is included in the U 5f states in the calculations. This leads to a marked increase of especially the orbital moment μ_l on the U site and, hence, also its value of the ordered magnetic moment, which becomes as large as $-1.41\ \mu_{\mathrm{B}}$ compared with the total moment of $-1.95\ \mu_{\mathrm{B}}$ for the c axis. A similar situation also occurs for the remaining axes. It is quite obvious that this enhancement, compared with the available experimental results that indicate very weak ferromagnetism [1–3], is completely unsupported. Moreover, this finding agrees with our experience that OPC applied to the 5f electrons usually strongly overestimates the values of uranium ordered magnetic moments. As our calculations indicate, the difference in energy between the non-magnetic and ferromagnetic LSDA ground states for the c axis is lower by 3 mhartree. This is quite small, and it may certainly cause some difficulties in stabilizing a long-range ferromagnetic state, the more so with such a small value of the experimentally determined ordered magnetic moments as the $0.07\ \mu_{\mathrm{B}}$ reported in [3]. Thus, this may lead only to

Table 6. Values of ordered spin (μ_s), orbital (μ_l) and total (μ_{tot}) magnetic moments in μ_B for the ferromagnetic arrangement of moments directed along the *a*, *b* and *c* axes, respectively.

Approximations		LSDA				LSDA + OPC			
Axis	Atomic positions	μ_s	μ_l	μ_s/μ_l	μ_{tot}	μ_s	μ_l	μ_s/μ_l	μ_{tot}
a	U	1.012	−0.919	−0.908	0.093	1.228	−2.560	−2.085	−1.332
	Co	−0.230	−0.062	0.270	−0.292	−0.311	−0.177	0.569	−0.488
	Ge	−0.038	−0.002	0.053	−0.040	−0.053	−0.010	0.189	−0.063
	per f.u.	0.744	−0.983	−1.321	−0.239	0.864	−2.747	−3.179	−1.883
b	U	1.063	−1.156	−1.088	−0.093	1.273	−2.731	−2.145	−1.458
	Co	−0.227	−0.063	0.278	−0.290	−0.317	−0.188	0.593	−0.505
	Ge	−0.038	−0.001	0.026	−0.039	−0.050	−0.011	0.220	−0.061
	per f.u.	0.798	−1.219	−1.528	−0.421	0.906	−2.930	−3.234	−2.024
c	U	1.076	−1.215	−1.129	−0.139	1.254	−2.666	−2.126	−1.412
	Co	−0.231	−0.057	0.247	−0.288	−0.300	−0.183	0.610	−0.483
	Ge	−0.036	−0.002	0.056	−0.038	−0.045	−0.010	0.222	−0.055
	per f.u.	0.809	−1.274	−1.575	−0.465	0.909	−2.859	−3.145	−1.950

magnetic fluctuations, which are partly frozen by application of a magnetic field.

Furthermore, in UCoGe the calculated (by FPLO5-LDA) total and partial atomic contributions to XPS are compared with our experimental valence XPS measured in the paramagnetic state (i.e. at room temperature) and are displayed in figure 10. The experimental background was subtracted from the XPS spectrum using the Tougaard method [23]. As seen in figure 10, the calculated total spectrum for an energy resolution of 0.3 eV has a more complex structure than the experimental one, which is usually not well resolved. It is interesting to note that the peak closest to E_F, numbered 1, is split at its top into two narrow peaks. One of them, crossing E_F, is the highest in the whole valence spectrum. It originates mainly from a large contribution of the U $5f_{5/2}$ electrons, which are dominating in the spectrum down to about 1 eV binding energy. It is interesting to mention that for the cases of energy resolution of 0.4 and 0.6 eV (not displayed here) this double splitting becomes either flatter or completely rounded, respectively. The whole peak 1 also contains a tail contribution from the Co 3d electrons, participating in a metallic bond. The second peak, occurring in the range of 1–5.5 eV binding energy, is broad and centred at 2 eV below E_F. It consists of the Co 3d electron contributions, dominating in this energy region, and strongly hybridizing with a twice-smaller intensity contribution stemming from the U 5f electrons. The third peak, composed mainly of the Ge 4s electrons, exists in the range of 8–10 eV and has a rather small intensity. In turn, the U 6d electron contribution, visible in the DOS in figure 4, is completely diminished by the photoionization cross-sections and cannot be detected by the XPS measurements. For the same reason, the Ge 4p electrons are also only slightly visible in the energy range of 2–5 eV binding energy.

As figure 10 indicates, the experimental XPS spectrum seems to be more smeared in energy and less structured in comparison with the theoretical one. First of all, the first and second peaks are not so clearly separated from each other. The rounded top of the experimental U 5f peak is markedly shifted from E_F towards higher binding energies compared with the theoretical weighted prediction. Hence, the U 5f electrons might be somewhat more localized from the point

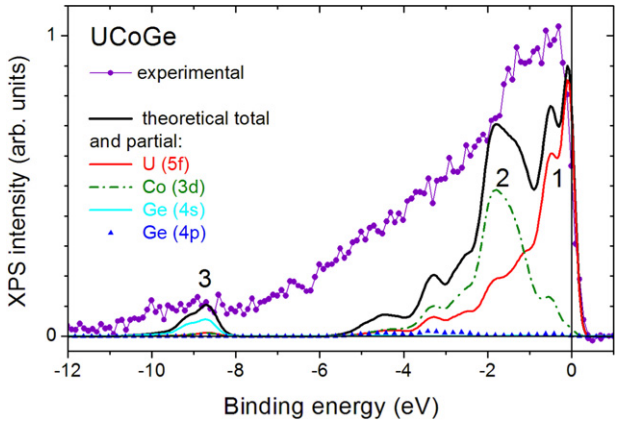

Figure 10. Experimental total valence band XPS spectrum of UCoGe in the paramagnetic state, compared with the calculated non-magnetic (LDA) total spectrum and its partial contributions (originating from different electronic states), convoluted with a Gaussian simulating experimental energy resolution of 0.3 eV.

of view of the experimental spectrum. At the same time, the experimental Co 3d electron peak is reduced and slightly shifted towards E_F with respect to the theoretical one. The third peak obtained in the calculations is well reproduced by the experiment. The lack of the pronounced O (2s) contribution at about 6 eV below E_F indicates rather low contamination of the sample by oxygen. These XPS spectra exhibit either mostly delocalized character of the U 5f electrons or, completely the opposite, some expanded multiplet structure coming from some localized character of 5f states owing to their quite broad contribution ranging down to about 5 eV binding energy.

Our experimental U 4f core lines measured in the paramagnetic state of UCoGe at room temperature are presented in figure 11.

They are decomposed by using the Doniach–Šunjić theory [24] (the background here is also subtracted by the Tougaard method [23]), into two highly asymmetric $4f_{5/2}$ (−388.2 eV) and $4f_{7/2}$ (−377.4 eV) main sublines, split by 10.8 eV owing to the spin–orbit interaction. Since the U $4f_{5/2}$ subline is somewhat overlapped by a plasmon, only the U

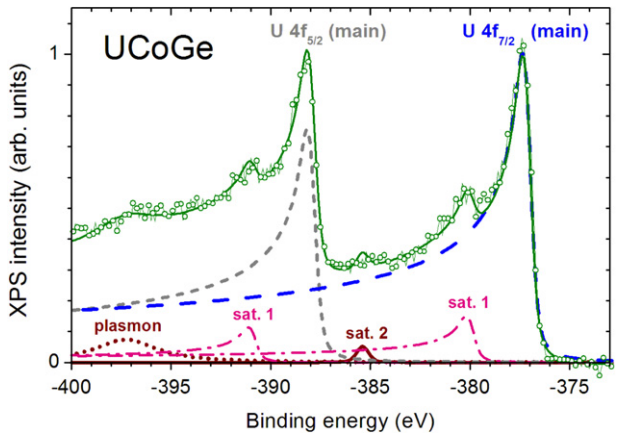

Figure 11. Experimental XPS spectrum of the U 4f core electron lines in UCoGe in the paramagnetic state (marked by lines with circles). The spectrum is decomposed (by a deconvolution procedure) into the main sublines $4f_{5/2}$ and $4f_{7/2}$ (denoted by dashed and short-dashed lines) and their satellites (dashed–dotted or solid lines labelled as sats 1 and 2) as well as a single plasmon contribution.

$4f_{7/2}$ subline can be subject to an interpretation. As seen in figure 11, the U $4f_{7/2}$ subline is accompanied by two peaks, namely, a distinct 3 eV satellite (sat. 1) and a small intensity 7 eV satellite (sat. 2), centred at −380.2 eV and −385.4 eV, respectively. Thus, in this case, inferring any information on the initial and final states in the photoemission processes becomes more difficult. Evidence of the 3 eV satellite may point to an additional final state of the U $5f^3$ kind, indicating for example a dualism of 5f electrons, the more so as the satellite is highly asymmetric. However, one cannot exclude some small intensity contamination by uranium oxides such as UO_2 [25] in this energy region, although, as experiment shows, there is only a negligible trace of the O (KLL) peak in the overall XPS spectrum (not presented here) and no clear evidence of the oxygen peak at about 6 eV binding energy in the valence band and the lack of symmetry of the 3 eV satellite. Finally, the very small 7 eV satellite, usually occurring in many other uranium compounds, is commonly ascribed to some evidence of localization of the U 5f electrons. Its smallness in the core-level XPS spectrum is consistent with the rather delocalized nature of the 5f electrons deduced from the valence band XPS.

5. Discussion

As mentioned in section 1, two theoretical papers on the electronic structure of UCoGe have already been published [10, 11]. In this compound, as in many other intermetallic uranium compounds, the spin–orbit coupling of the U 5f states is strong (of the order of 1 eV), thus only results obtained in fully relativistic calculations are reasonable. In the paper by Diviš [10] such results, obtained by the WIEN2k code, have been presented in figure 3 of [10], showing total DOSs in the ferromagnetic state (with the moment along the c axis) but without presenting separate spin-up and spin-down channels. In general, our FPLO results, displayed in figure 5, are in overall quite good agreement with the previous results [10] (note that the magnitudes of DOSs in our paper are in units per f.u. and not per u.c. = 4 f.u.). However, some differences occur, mainly around E_F. They are likely due to a better (direct) evaluation of the spin–orbit coupling and achieving higher accuracy owing to a much denser k-mesh of 1728 points (compared with 200) and apparently also a denser energy mesh used in our FPLO calculations with respect to the WIEN2k results in [10]. As shown in figure 5, E_F cuts the DOSs at a minimum, which (as has been checked by us but the results are not displayed here) is not the case when using a less dense energy mesh and, hence, this feature is not seen in figure 3 of [10]. As a consequence, the electronic specific heat coefficient γ_b calculated by us is somewhat smaller than that reported by Diviš (8.1 versus 12.7 mJ K^{-2} mol^{-1}) and both values are several times smaller than the experimental value of 57 mJ K^{-2} mol^{-1} reported in [1]. Furthermore, our calculations reveal two high intensity peaks of the U 5f states just below E_F, which are not seen in figure 3 of the paper [10], that may be responsible for magnetic instabilities and fluctuations in UCoGe, as is the case in RCo_2-type compounds [20].

In turn, the authors of [11] also present in their figure 2 fully relativistic results obtained by the WIEN2k code, namely the total DOSs and U 5f contributions, split into spin-up and spin-down channels, for UCoGe in the ferromagnetic state (along the c axis). In that figure, the case without the Hubbard U_H term gives better agreement with the experimental magnetic moment and corresponds to our data presented in figure 6, that are more detailed and better resolved. It appears further that our results are in satisfying agreement with the results of figure 2 of [11]. In both cases E_F cuts the DOSs at their minimum and the spin-down channels even have a pronounced pseudogap at E_F, causing UCoGe to exhibit almost half-metallic properties. Nevertheless, there is a slight difference between our and the previous results [11] in the magnitude of the peaks below E_F mentioned above, which have much smaller intensities in the previous results [11] obtained on a less dense k-mesh (of 462 points) and probably also on a less dense energy mesh. Moreover, we show explicitly other contributions of valence electronic states to the total DOS. It is clearly visible in figure 6 that the exchange splitting concerns not only the U 5f but also the Co 3d electrons. These U and Co electrons hybridize at E_F and also with the U 6d and Ge 4p ones. With respect to the previously reported calculations [10, 11], we additionally present in figure 3 selected band weights (for both non-magnetic and ferromagnetic cases) showing pronounced weighted contributions of the U $5f_{5/2}$ electrons to bands at E_F, which are well separated from the U $5f_{7/2}$ states shifted above E_F. It is well seen just in this figure that the Co 3d states have a pronounced contribution to bands in the whole displayed energy range and, hence, also hybridize with all U 5f states. Our DOSs presented also in the non-magnetic case in figure 4 have slightly lower values at E_F and a pseudogap at −0.2 eV compared with the ferromagnetic case presented in figure 6. In addition, we display in figure 2 band energies and in figure 7 the Fermi surfaces for both non-magnetic and ferromagnetic states, showing that in the former state UCoGe

has semimetallic character with possible FS nesting along the *c* axis, while in the latter state it exhibits typically metallic bands and an FS with nesting properties along all three axes, which may support both ferromagnetic and superconducting states in this compound. As seen in figure 7, the FS of UCoGe in the non-magnetic state exists in three Kramers double degenerated bands, while that in the ferromagnetic state occurs in four non-degenerated bands. The shape of the total ferromagnetic FS of UCoGe, obtained employing the WIEN2k code, is displayed in figure 5 of [11]. It was determined apparently with a poor resolution in the **k**-space and adopting a non-fully-relativistic convention such that the spin-up and spin-down sheets are drawn separately. It is clearly visible from the figure that the spin-down FS sheets are quite small, making it easy to imagine that the total non-separated FS should have a very different shape from our total one (containing sheets from all bands). Our ferromagnetic FS shows explicitly that UCoGe could be a multiband ferromagnetic superconductor.

The present total energy calculations show that the ferromagnetic state of UCoGe is a little more stable (slightly lower in total energy) than the non-magnetic one, which also confirms the results reported in papers [10, 11]. Furthermore, the ferromagnetic arrangement along the *c* axis is more favourable than that along the *b* and *a* axes. This is also in good agreement with the WIEN2k results of [11]. The authors of the latter paper have also ruled out the possibility of any non-collinear magnetic ordering existing. According to table 6, our absolute value of total magnetic moments in the ferromagnetic state along the *c* axis (within LSDA) amounts to 0.465 μ_B (per f.u.), somewhat lower than that reported in [11] (0.633 μ_B), and both values are comparable to that reported in [10], while the experimental magnetic moment is only equal to 0.07 μ_B [3]. As to the values of the magnetic moment considered solely on a uranium atom in UCoGe, we observe (see table 6) almost a complete cancellation of its antiparallel spin and orbital contributions, both having an absolute magnitude of about 1 μ_B, which yields the total moment per U atom of only 0.1 μ_B, in close agreement with the results of both previous theoretical papers [10, 11]. However, our values of magnetic moments per U atom for the *c* axis (table 6) are rather closer to those reported in [11] than to those in [10]. This stems from the fact that the calculated total moment on the U atom was found (see table 6) to have a negative sign, being opposite to that reported by Diviš [10]. In turn, the spin and orbital moment contributions connected with Co, being parallel to each other, are also negative, and the total value on the Co atom is roughly twice as high as that of the parallel magnetic moment on the U atom. In fact, this means that the net ferromagnetic moment in UCoGe originates mainly from the Co rather than from the U atom, which should be specially underlined. This agrees well with the results of [11] and, despite the difference in the sign, also with [10]. There are only differences in magnitudes of the total Co magnetic moments, ranging from -0.25 μ_B [10] to -0.53 μ_B [11], depending on the calculation method used. We obtained a value of only -0.29 μ_B, which is close to the former one, obtained by employing the same FPLO method but adopting slightly different lattice parameters and probably also atomic positions (not given). In the case of our results and those reported in [11], the U and Co total magnetic moments are parallel, in contrast to those reported by Diviš [10]. Based on our results and those reported in [11], the idea of superconductivity formed by triplet pairing mediated by ferromagnetic fluctuations [1] becomes more probable. The singlet scenario would be possible in the case of the ferromagnetic arrangement but along the *a* axis, for which the total moments on U and Co atoms are predicted to be antiparallel by both our calculations and those in [11]. However, in contrast to two previous papers [10, 11], we also give occupation numbers *N* of valence electronic states and observe their strong enhancement compared with *N* in free atoms in the case of d and p valence electrons. The substantial changes are as follows: for the U 6d, from $N = 1$ to 2.38; Co 3d, from 7 to 8; U 7p, from 0 to 0.22; Co 4p, from 0 to 0.74, and Ge 4p, from 2 to 2.19. Finally, it is interesting to mention that our room-temperature XPS 4f core results suggest a possibility of some dualism, i.e. both itinerant and localized character of the U 5f electrons. It would be interesting to have the opportunity to compare our dHvA theoretical results with some experimental data, which unfortunately are not available yet. However, a large interest focused on this compound currently allows one to assume that it may be done soon after obtaining much purer single crystals.

6. Conclusions

The crystal and electronic structures of UCoGe have been investigated by x-ray diffraction on a single crystal, and FPLO band structure calculations based on these diffraction results. The theoretical electronic densities of states were examined by the XPS measurements. Fair agreement is achieved between the experimental and theoretical XPS results for the paramagnetic state. A small difference in the position of the U 5f electron states is observed, which points to a slightly higher localization of the U 5f states at room temperature seen in the experiment. However, some discrepancy also exists for the Co 3d electron contributions. Considering the paramagnetic Fermi surface, we have found it to be typical of a semimetal, while the ferromagnetic one, corresponding to a small magnetic moment of -0.47 μ_B/f.u. along the *c* axis, exhibits more metallic properties, with nesting propensities that may favour superconductivity.

Acknowledgments

We are grateful to J Stępień-Damm and B Coqblin for their interest in this paper. We also thank U Nitzsche at IFW Dresden for technical assistance with the IFW computers.

References

[1] Huy N T, Gasparini A, de Nijs D E, Huang Y, Klaasse J C P, Gortenmulder T, de Visser A, Hamann A, Görlach T and Löhneysen H v 2007 *Phys. Rev. Lett.* **99** 067006
[2] de Nijs D E, Huy N T and de Visser A 2008 *Phys. Rev.* B **77** 140506(R)
[3] Huy N T, de Nijs D E, Huang Y K and de Visser A 2008 *Phys. Rev. Lett.* **100** 077002

[4] Troć R and Tran V H 1988 *J. Magn. Magn. Mater.* **73** 389
[5] Canepa F, Manfrinetti P, Pani M and Palenzona A 1996 *J. Alloys Compounds* **234** 225
[6] Lloret B 1988 *PhD Thesis* University Bordeaux I
[7] Buschow K H J, Brück E, van Wierst R G, de Boer F R, Havela L, Sechovsky V and Nozar P 1990 *J. Appl. Phys.* **67** 5215
[8] Ohta T, Nakai Y, Ihara Y, Ishida K, Deguchi K, Sato N K and Satoh I 2008 *J. Phys. Soc. Japan* **77** 023707
[9] Hassinger E, Aoki D, Knebel G and Flouquet J *J. Phys. Soc. Japan* **77** 073703
[10] Diviš M 2008 *Physica* B **403** 2505
[11] de la Mora P and Navarro O 2008 *J. Phys.: Condens. Matter* **20** 285221
[12] FPLO-5.00-18 and 5.10-20 improved version of the original FPLO code by Koepernik K and Eschrig H 1999 *Phys. Rev.* B **59** 1743 http://www.FPLO.de
[13] Eschrig H, Richter M and Opahle I 2004 *Relativistic Electronic Structure Theory: Applications* Part II ed P Schwerdtfeger (Amsterdam: Elsevier) pp 723–76
[14] Sheldrick G M 1997 *SHELX-97, Program for Crystal Structure Refinement* (Germany: University of Göttingen)
[15] Talik E, Lucas M-E, Suski W and Troć R 2003 *J. Alloys Compounds* **350** 72
[16] Perdew J P and Wang Y 1992 *Phys. Rev.* B **45** 13244
[17] Eriksson O, Brooks M S S and Johansson B 1990 *Phys. Rev.* B **41** 7311
Carsten N 2007 Orbital polarization corrections in relativistic density functional theory, OPC implementation in FPLO5.10-20 *Diploma Thesis* (Dresden: Technische Universität) http://www.ifw-dresden.de/institutes/itf/diploma-and-phd-theses-at-the-itf
[18] Yeh J J and Lindau I 1985 *At. Data Nucl. Data Tables* **32** 1
[19] Oppeneer P M and Lodder A 1987 *J. Phys. F: Met. Phys.* **17** 1901
[20] Yamada H 1988 *Physica* B **149** 390
[21] Dugdale S B, Fretwell H M, Alam M A, Kontrym-Sznajd G, West R N and Badrzadeh S 1997 *Phys. Rev. Lett.* **79** 941
Biasini M, Kontrym-Sznajd G, Monge M A, Gemmi M, Czopnik A and Jura A 2001 *Phys. Rev. Lett.* **86** 4616
Hughes D, Däne M, Ernst A, Hergert W, Lüders M, Poulter J, Staunton J B, Svane A, Szotek Z and Temmerman W M 2007 *Nature* **446** 650
[22] Elgazzar S, Opahle I, Hayn R and Oppeneer P M 2004 *Phys. Rev.* B **69** 214510
[23] Tougaard S 1990 *J. Electron Spectrosc. Relat. Phenom.* **52** 243
[24] Doniach S and Šunjić M 1970 *J. Phys. C: Solid State Phys.* **3** 285
[25] Grohs H, Höchst H, Steiner P, Hüfner S and Buschow K H J 1980 *Solid State Commun.* **33** 573